Exploring the evolution of stellar rotation using Galactic kinematics

Ruth Angus[1,2,3], Angus Beane[4], Adrian M. Price-Whelan[2], Jason Curtis[1], Travis Berger[6], Rocio Kiman[7], Elisabeth Newton[5], Jennifer van Saders[6], Dan Foreman-Mackey[2], Yuxi Lu[1], 3, Lauren Anderson[8]

ABSTRACT

[1]American Museum of Natural History, Central Park West, Manhattan, NY, USA

[2]Center for Computational Astrophysics, Flatiron Institute, 162 5th Avenue, Manhattan, NY, USA

[3]Department of Astronomy, Columbia University, Manhattan, NY, USA

[4]Harvard-Smithsonian Center for Astrophysics, Cambridge, MA, USA

[7]Department of physics, CUNY Graduate Center, City University of New York, Manhattan, NY, USA

[6]Institute for Astronomy, University of Hawai'i at Mānoa, Honolulu, HI, USA

[5]Dartmouth College, Hanover, NH, USA

[8]Carnegie Observatories, Pasadena, CA, USA

The rotational evolution of cool dwarfs is poorly constrained after ∼1-2 Gyr due to a lack of precise ages and rotation periods for old main-sequence stars. In this work, we use the velocity dispersions of low-mass *Kepler* dwarfs as an age proxy, to reveal their rotational evolution and demonstrate that kinematics could be a useful tool for calibrating gyrochronology. We find that a gyrochronology model, calibrated to fit the period–$T_{\rm eff}$ relationship of the Praesepe cluster, does not apply to stars older than around 1 Gyr. Although late-K dwarfs spin more slowly than early-K and late-G dwarfs when they are young, at old ages we find that late-G and early-K dwarfs rotate at the *same rate* or faster than late-K dwarfs of the same age. This result agrees qualitatively with semi-empirical models that vary the rate of surface-to-core angular momentum transport as a function of time and mass. It also aligns with recent observations of stars in the NGC 6811 cluster, which indicate that K dwarfs experience an epoch of stalled spin-down. We find that the oldest *Kepler* stars with measured rotation periods are late-K and early-M dwarfs, indicating that these stars maintain spotted surfaces and stay magnetically active longer than more massive stars. Finally, based on their kinematics, we confirm that many rapidly rotating K-dwarfs are likely to be synchronized binaries.

1. Introduction

1.1. Gyrochronology

Stars with significant convective envelopes ($\lesssim 1.3$ $M_\odot$) have strong magnetic fields and slowly lose angular momentum via magnetic braking (*e.g.* Schatzman 1962; Weber and Davis 1967; Skumanich 1972; Kawaler 1988; Pinsonneault et al. 1989). Although stars are born with random rotation periods, between 1 and 10 days, observations of young open clusters reveal that their rotation periods converge onto a unique sequence by ∼500-700 million years (*e.g.* Irwin and Bouvier 2009; Gallet and Bouvier 2013). After this time, the rotation period of a star is thought to be determined, to first order, by its color and age alone. This is the principle behind gyrochronology, the method of inferring a star's age from its rotation period (*e.g.* Barnes 2003, 2007, 2010; Meibom et al. 2011, 2015). However, new photometric rotation periods made available by the *Kepler* (Borucki et al. 2010) and *K2* (Howell et al. 2014) missions (*e.g.* McQuillan et al. 2014; García et al. 2014; Douglas et al.

2017; Rebull et al. 2017; Meibom et al. 2011, 2015; Curtis et al. 2019) have revealed that rotational evolution is more complicated than previously thought. For example, the early-to-mid M dwarfs in the $\sim$ 650 Myr Praesepe cluster spin more slowly than the G dwarfs; in theory because lower-mass stars have deeper convective zones which generate stronger magnetic fields and more efficient magnetic braking. However, in the NGC 6811 cluster which is around 1.1 Gyr (Janes and Hoq 2011), late-K dwarfs rotate at the *same rate* as early-K dwarfs (Curtis et al. 2019). In other words, convection zone depth cannot be the only variable that affects stellar spin-down rate. New semi-empirical models that vary the rate of angular momentum redistribution in the interiors of stars are able to reproduce this flattened period–color relation (Spada and Lanzafame 2019). These models suggest that mass and age-dependent angular momentum transport between the cores and envelopes of stars has a significant impact on their surface rotation rates. Another example of unexpected rotational evolution is seen in old field stars which appear to rotate more rapidly than classical gyrochronology models predict (Angus et al. 2015; van Saders et al. 2016, 2018; Metcalfe and Egeland 2019). A mass-dependent modification to the classical $P_{\rm rot} \propto t^{\frac{1}{2}}$ spin-down law (Skumanich 1972) is required to reproduce these observations. To fit magnetic braking models to these data, a cessation of magnetic braking is required after stars reach a Rossby number (Ro; the ratio of rotation period to convective turnover time) of around 2 (van Saders et al. 2016, 2018).

The rotational evolution of stars is clearly a complicated process and, to fully calibrate the gyrochronology relations we need a large sample of reliable ages for stars spanning a range of ages and masses. In this paper, we use the velocity dispersions of field stars to qualitatively explore the rotational evolution of GKM dwarfs, and show that kinematics could provide a gyrochronology calibration sample.

1.2. Using kinematics as an age proxy

Stars are thought to be born in the thin disk of the Milky Way (MW), orbiting the Galaxy with a low out-of-plane, or vertical, velocity ($v_{\mathbf{z}}$), just like the star-forming molecular gas observed in the disk today (*e.g.* Stark and Brand 1989; Stark and Lee 2005; Aumer and Binney 2009; Martig et al. 2014; Aumer et al. 2016). On average, the vertical velocities of older stars is observed to be larger (*e.g.* Nordström et al. 2004; Holmberg et al. 2007, 2009; Aumer and Binney 2009; Casagrande et al. 2011). This is likely either a signature of dynamical heating, such as from interactions with giant molecular clouds, spiral arms and the galactic bar (see Sellwood 2014, for a review of secular evolution in the MW), or an indication that stars formed dynamically "hotter" in the past (e.g., Bird et al. 2013). In either case,

the vertical velocity distribution is observed to depend significantly on stellar age. While the velocity of any individual star only provides a weak age constraint, because its velocity depends on its current position in its orbit, the velocity *dispersion* of a *group* of stars indicates whether that group is old or young relative to other groups. In this work, we compare the velocity dispersions of groups of field stars in the Galactic thin disk to ascertain which groups are older and which younger, and draw conclusions about the rotational evolution of stars based on their implied relative ages.

Although *vertical* velocity, $v_{\mathbf{z}}$, is an established age proxy, it can only be calculated with full 6-dimensional position and velocity information. In fact, with full 6D phase space and an assumed Galactic potential, it is possible to calculate the dynamically-invariant vertical *action*, which may be an even better age indicator (Beane et al. 2018; Ting and Rix 2019). Unfortunately, most field stars with measured rotation periods do not have radial velocity (RV) measurements because they are relatively faint *Kepler* targets (∼12th-16th magnitudes). For this reason, we used velocity in the direction of galactic latitude, $v_{\mathbf{b}}$, as a proxy for $v_{\mathbf{z}}$. The *Kepler* field is positioned at low galactic latitude (b=∼5-20°), so $v_{\mathbf{b}}$ is a close (although imperfect, see appendix) approximation to $v_{\mathbf{z}}$. Because we use $v_{\mathbf{b}}$ rather than $v_{\mathbf{z}}$ we do not calculate absolute kinematic ages using a published age–velocity dispersion relation (AVR), calibrated with vertical velocity. In future it may be possible to account for the differences between $v_{\mathbf{b}}$ and $v_{\mathbf{z}}$, or marginalize over missing RV measurements and the *Kepler* selection function, in order to infer absolute ages. Regardless of direction however, velocity dispersion is expected to monotonically increase over time (*e.g.* Holmberg et al. 2009), and can therefore be used to *rank* groups of stars by age.

This paper is laid out as follows: in section 2 we describe our sample selection process and the methods used to calculate stellar velocities. In section 3 we use kinematics to investigate the relationship between stellar rotation period, age and color/$T_{\rm eff}$ and interpret the results. We also examine the rotation period gap and the kinematics of synchronized binaries. In the appendix, we establish that $v_{\mathbf{b}}$ velocity dispersion, $\sigma_{v\mathbf{b}}$, can be used as an age proxy by demonstrating that neither mass-dependent heating nor the *Kepler*/*Gaia* selection function is observed to strongly affect our sample.

2. Method

2.1. The data

We used the publicly available *Kepler*-*Gaia* DR2 crossmatched catalog[9] to combine the McQuillan et al. (2014) catalog of stellar rotation periods, measured from *Kepler* light curves, with the *Gaia* DR2 catalog of parallaxes, proper motions and apparent magnitudes. Reddening and extinction from dust was calculated for each star using the Bayestar dust map implemented in the `dustmaps` *Python* package (M. Green 2018), and `astropy` (Astropy Collaboration et al. 2013; Price-Whelan et al. 2018).

For this work, we used the precise *Gaia* DR2 photometric color, $G_{\rm BP} - G_{\rm RP}$, to estimate $T_{\rm eff}$ for the Kepler rotators. Curtis *et al.* (2020, in prep) combined effective temperature measurements for nearby, unreddened field stars in benchmark samples, including FGK stars characterized with high-resolution optical spectroscopy (Brewer et al. 2016), M dwarfs characterized with low-resolution optical and near-infrared spectroscopy (Mann et al. 2015), and K and M dwarfs characterized with interferometry and bolometric flux analyses (Boyajian et al. 2012). This empirical color–temperature relation is valid over the color range $0.55 < (G_{\rm BP} - G_{\rm RP})_0 < 3.20$, corresponding to $6470 < T_{\rm eff} < 3070$ K. The dispersion about the relation implies a high precision of 50 K. These benchmark data enable us to accurately estimate $T_{\rm eff}$ for cool dwarfs (*e.g.* Rabus et al. 2019), and allows us to correct for interstellar reddening at all temperatures[10]. The equation we used to calculate photometric temperatures from Gaia $G_{BP} - G_{RP}$ color is a seventh-order polynomial with coefficients given in table 1.

Photometric binaries and subgiants were removed from the McQuillan et al. (2014) sample by applying cuts to the color-magnitude diagram (CMD), shown in figure 1. A 6th-order polynomial was fit to the main sequence and raised by 0.27 dex to approximate the division between single stars and photometric binaries (shown as the curved dashed line in figure 1). All stars above this line were removed from the sample. Subgiants were also removed by eliminating stars brighter than 4th magnitude in *Gaia* G-band.

The rotation periods of the dwarf stars in the McQuillan et al. (2014) sample are shown on a *Gaia* color-magnitude diagram (CMD) in the top panel of figure 1. In the bottom panel, the stars are colored by their gyrochronal age, calculated using the Angus et al.

[9]Available at gaia-kepler.fun

[10]The color–temperature relation is described in detail in the Appendix of, and the formula is provided in Table 4 of, Curtis *et al.* (2020, in prep).

Table 1: Coefficient values for the 7th-order polynomial used to estimate $T_{\rm eff}$ from *Gaia* $G_{BP} - G_{RP}$ color, calibrated in Curtis *et al.* (2020, in prep).

$(G_{BP} - G_{RP}$) exponent	Coefficient
0	-416.585
1	39780.0
2	-84190.5
3	85203.9
4	-48225.9
5	15598.5
6	-2694.76
7	192.865

(2019) gyrochronology relation. The stars with old gyrochronal ages, plotted in purple hues, predominantly lie along the upper edge of the MS, where stellar evolution models predict old stars to be, however the majority of these 'old' stars are bluer than $G_{BP} - G_{RP} \sim 1.5$ dex. The lack of gyrochronologically old M dwarfs suggests that either old M dwarfs are missing from the McQuillan et al. (2014) catalog, or the Angus et al. (2019) gyrochronology relation under-predicts the ages of low-mass stars. Given that lower-mass stars stay active for longer than higher-mass stars (*e.g.* West et al. 2011; Kiman et al. 2019), and are therefore more likely to have measurable rotation periods at old ages, the latter scenario seems likely. However, it is also possible that the rotation periods of the oldest early M dwarfs are so long that they are not measurable with Kepler data. Ground-based rotation period measurements of mid and late M dwarfs indicate that there is an upper limit to the rotation periods of *late* M dwarfs of around 140 days (Newton et al. 2016, 2017, 2018), which is much longer than the longest rotation periods measured in the McQuillan et al. (2014) sample (around 70 days). The apparent lack of old ages for M dwarfs in figure 1 may be caused by a combination of ages being underestimated by a poorly calibrated model, and rotation period detection bias. The Angus et al. (2019) gyrochronology relation is a simple polynomial model, fit to the period-color relation of Praesepe. Inaccuracies are a typical feature of empirically calibrated gyrochronology models: since there are no (or at least very few) old M dwarfs with rotation periods, the models are poorly calibrated for these stars.

The `Pyia` (Price-Whelan 2018) and `astropy` (Astropy Collaboration et al. 2013; Price-Whelan et al. 2018) *Python* packages were used to calculate velocities for the McQuillan et al. (2014) sample. `Pyia` calculates velocity samples from the full *Gaia* uncertainty covariance matrix via Monte Carlo sampling, thereby accounting for the covariances between *Gaia* positions, parallaxes and proper motions. Stars with negative parallaxes, parallax

Fig. 1.— Top: de-reddened MS *Kepler* stars with McQuillan et al. (2014) rotation periods, plotted on a *Gaia* CMD. We removed photometric binaries and subgiants from the sample by excluding stars above the dashed lines. Bottom: a zoom-in of the top panel, with stars colored by their gyrochronal age (Angus et al. 2019), instead of their rotation period. A general age gradient is visible across the main sequence. Since the Angus et al. (2019) relation predicts that the oldest stars in the McQuillan et al. (2014) sample are late-G and early-K dwarfs, it is probably under-predicting the ages of late-K and early-M dwarfs.

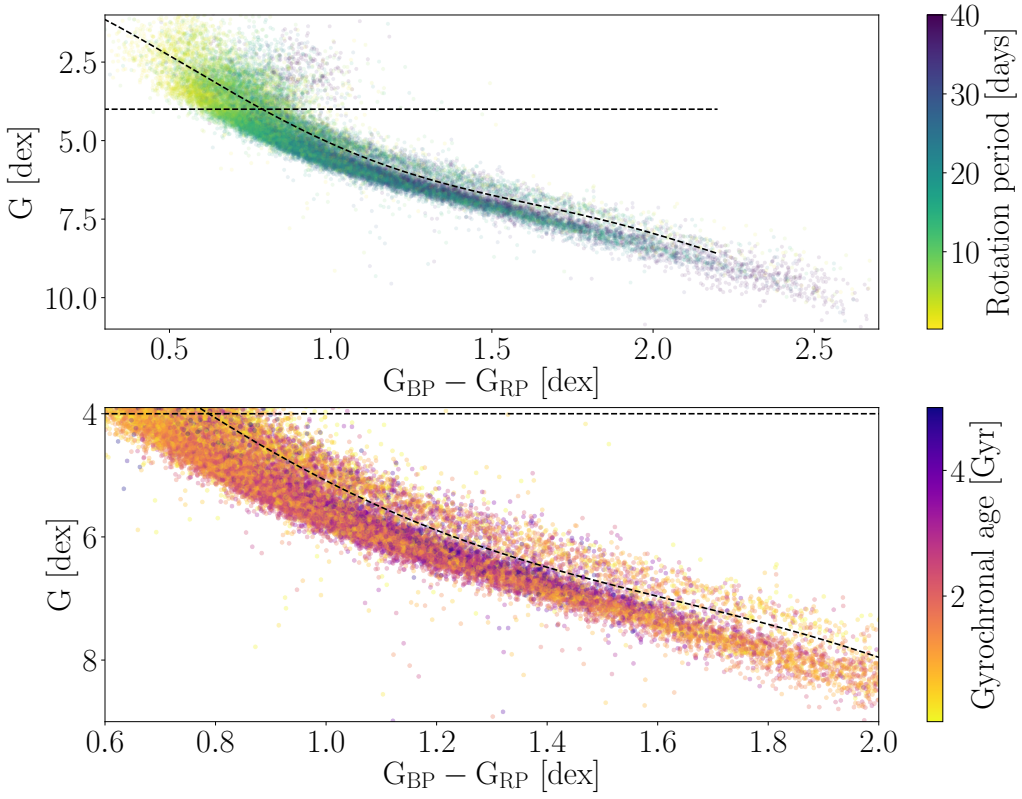

signal-to-noise ratios less than 10, stars fainter than 16th magnitude, stars with absolute $v_{\mathbf{b}}$ uncertainties greater than 1 kms^{-1} and stars with galactic latitudes greater than 15° (justification provided below) were removed from the sample. Finally, we removed stars with rotation periods shorter than the main population of periods, since this area of the period-$T_{\rm eff}$ diagram is sparsely populated. We removed these rapid rotators by cutting out stars with gyrochronal ages less than 0.5 Gyr (based on the Angus et al. 2019, gyro-model), because a 0.5 Gyr gyrochrone[11] traces the bottom edge of the main population of rotation periods. After these cuts, around 13,000 stars out of the original ∼34,000 were included in the sample.

[11]A gyrochrone is a gyrochronological isochrone, or a line of constant age in period-$T_{\rm eff}$, or period-color space.

3. Results and Discussion

3.1. The period-$T_{\rm eff}$ relations, revealed

To explore the relationship between rotation period, effective temperature ($T_{\rm eff}$) and velocity dispersion, we calculated $\sigma_{v\mathbf{b}}$[12] for groups of stars with similar rotation periods and temperatures, and presumed similar age. The top panel of figure 2 shows rotation period versus effective temperature for the McQuillan et al. (2014) sample, coloured by $\sigma_{v\mathbf{b}}$, where $\sigma_{v\mathbf{b}}$ was calculated for groups of stars over a grid in $\log_{10}$(period) and temperature. If we assume that mass dependent heating does not strongly affect this sample and $v_{\mathbf{b}}$ at low galactic latitudes is an unbiased tracer of $v_{\mathbf{z}}$, then $v_{\mathbf{b}}$ velocity dispersion can be interpreted as an age proxy, and stars plotted in a similar color in figure 2 are similar ages. We discuss this assumption further in the appendix.

Overall, figure 2 shows that velocity dispersion increases with rotation period across all temperatures, implying that rotation period increases with age, as expected. This result is insensitive to the choice of bin position and size. Black lines show gyrochrones from the Angus et al. (2019) gyrochronology model, which projects the rotation-color relation of Praesepe to longer rotation periods over time. These gyrochrones are plotted at 0.5, 1, 1.5, 2, 2.5, 4 and 4.57 Gyr. At the youngest ages, these gyrochrones describe the data well: the palest yellow (youngest) stars with the lowest velocity dispersions all fall close to the 0.5 Gyr gyrochrone. However, although the 0.5 Gyr and 1 Gyr gyrochrones also trace constant velocity dispersion/age among the field stars, by 1.5 Gyr the gyrochrones start to *cross* different velocity dispersion regimes. For example, the 1.5 Gyr gyrochrone lies on top of stars with velocity dispersions of around 10-11 kms^{-1} at 5000-5500K and stars with $\sim$15 kms^{-1} velocity dispersions at 4000-4500K. The gyrochrones older than 1.5 Gyr also cross a range of velocity dispersions. If these were true isochrones they would follow lines of constant velocity dispersion. At ages older than around 1 Gyr, it appears that gyrochrones should have a more flattened, or even inverted, shape in rotation period-$T_{\rm eff}$ space than these Praesepe-based models.

The bottom panel of figure 2 shows velocity dispersion as a function of rotation period and *mass*, (from Berger et al. 2020), with gyrochrones from the (Spada and Lanzafame 2019) model shown in white. These gyrochrones are also plotted at 0.5, 1, 1.5, 2, 2.5, 4 and 4.57 Gyr. Each point plotted in the top panel also appears in the bottom panel with the same color. Because velocity dispersion was calculated in bins of $T_{\rm eff}$, not mass, bin outlines are clearly visible in the top panel but appear smeared-out in the bottom panel. In the bottom

[12] $\sigma_{v\mathbf{b}}$was calculated as 1.5$\times$ the median absolute deviation, to mitigate sensitivity to outliers.

Fig. 2.— Top: Rotation period vs effective temperature for stars in the McQuillan et al. (2014) sample, colored by the velocity dispersions of stars calculated over a grid in $\log_{10}$(period) and $T_{\rm eff}$. Black lines show gyrochrones from a gyrochronology model that projects the rotation-color relation of Praesepe to longer rotation periods over time (Angus et al. 2019). These gyrochrones do not appear to reflect the evolution of field stars at long rotation periods/old ages because they do not trace lines of constant velocity dispersion. Gyrochrones are plotted at 0.5, 1, 1.5, 2, 2.5, 4 and 4.57 Gyr in both top and bottom panels. Bottom: Same as top panel with rotation period vs *mass* (from Berger et al. 2020). White lines show gyrochrones from a model that includes mass and age-dependent angular momentum transport between the core and envelope (Spada and Lanzafame 2019). Qualitatively, these gyrochrones reflect the evolution of field stars at long rotation periods/old ages: they trace lines of constant velocity dispersion by reproducing periods of 'stalled' rotational evolution for K-dwarfs.

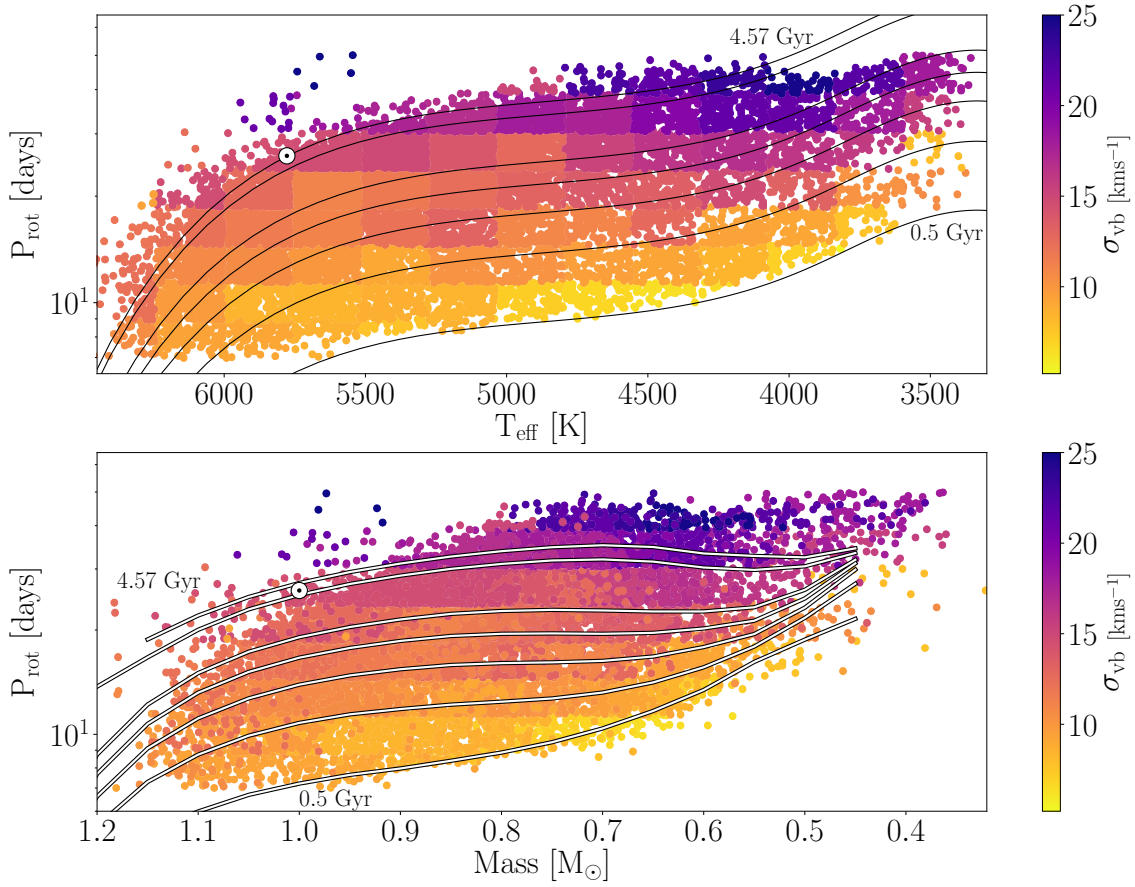

panel of figure 2, the Spada and Lanzafame (2019) models *do* trace lines of constant velocity dispersion, and reproduce the trends in the data at all ages. These models qualitatively agree with the data and reproduce the apparent flattening and inversion in the rotation period-$T_{\rm eff}$/mass relations.

The results shown in figure 2 indicate that stars of spectral type ranging from late G to late K (∼5500-3500 K) follow a braking law that changes over time. In particular, the relationship between rotation period and effective temperature appears to flatten out and eventually invert. These results provide further evidence for 'stalled' rotational evolution of K dwarfs, like that observed in open clusters (Curtis et al. 2019) and reproduced by models that vary angular momentum transport between stellar core and envelope with time and mass (Spada and Lanzafame 2019). The velocity dispersions of stars in the McQuillan et al. (2014) sample provide the following picture of rotational evolution. At young ages (younger than around 1 Gyr but still old enough to be on the main sequence and have transitioned from the 'I' sequence to the 'C' sequence Barnes 2003), stellar rotation period *decreases* with *increasing* mass. This is likely because lower-mass stars with deeper convection zones have stronger magnetic fields, larger Alfvén radii and therefore experience greater angular momentum loss rate (*e.g.* Schatzman 1962; Parker 1970; Kawaler 1988; Charbonneau 2010). According to the Spada and Lanzafame (2019) model, there is minimal transportation of angular momentum from the surface to the core of the star at these young ages, so the surface slows down but the core keeps spinning rapidly. This aligns with the current assumptions about stellar spin-down, dynamo theory, and the gyrochronology paradigm that has been in place for decades (*e.g.* Skumanich 1972; Noyes et al. 1984; Kawaler 1988; Barnes 2003; Angus et al. 2019). According to the data presented in figure 2 however, at intermediate ages, the rotation periods of K dwarfs appear *constant* with mass, and at late ages rotation period *increases* with *increaasing* mass. The interpretation of this, according to the Spada and Lanzafame (2019) model, is that lower-mass stars are still braking more efficiently at these intermediate and old ages but their cores are more tightly coupled to their envelopes, allowing angular momentum transport between the two layers. Angular momentum resurfaces and prevents the stellar envelopes from spinning-down rapidly, and this effect is strongest for late K-dwarfs with effective temperatures of ∼4000-4500K and masses ∼0.5-0.7 $M_\odot$.

It has been demonstrated that lower-mass stars remain magnetically active longer than more massive stars, (*e.g.* West et al. 2008; Kiman et al. 2019). If the detectability of a rotation period is considered to be a magnetic activity proxy, then our results provide further evidence for a mass-dependent activity lifetime. Figure 2 shows that the groups of stars with the largest velocity dispersions are cooler than 4500 K. This implies that the oldest stars with detectable rotation periods, are cooler than 4500 K, *i.e.* these-low mass stars stay active longer than more massive stars.

3.2. Synchronized binaries and the *Kepler* period gap

In this section, we explored the kinematic properties of the McQuillan et al. (2014) sample in more detail, investigating the velocity dispersions of stars either side of the *Kepler* period gap, and identifying rapidly rotating stars that may be synchronized binaries.

There is a sharp gap in the population of rotation periods (often called the *Kepler* period gap), which lies just above the 1 Gyr gyrochrone in the upper panel of figure 2, whose origin is unknown and is the subject of much speculation (McQuillan et al. 2014; Davenport and Covey 2018; Reinhold et al. 2019). This gap was first identified by McQuillan et al. (2014), and roughly follows a line of constant gyrochronal age of around 1.1 Gyr (according to the Angus et al. 2019, gyrochronology relation). Several explanations for the gap's origin have been proposed, including a discontinuous star formation history (McQuillan et al. 2013; Davenport 2017; Davenport and Covey 2018) and a change in magnetic field structure causing a brief period where rotational variability is reduced and rotation periods cannot be measured (Reinhold et al. 2019).

The top panel of figure 2 suggests that the Angus et al. (2019), Praesepe-based gyrochronology model is valid below the gap but not above. Gyrochrones follow lines of constant velocity dispersion below the gap, but *cross* lines of constant velocity dispersion above the gap. Although we do not provide an in-depth analysis here (and more data may be needed to confirm a connection) these data suggest that the gap may indeed separate a young regime where stellar cores are decoupled from their envelopes from an old regime where these layers are more tightly coupled. If so, this could indicate that the phenomenon responsible for changing the shape of gyrochrones in rotation-$T_{\rm eff}$ space is related to the phenomenon that produces the gap.

An alternate explanation for the gap is that the McQuillan et al. (2014) sample contains two distinct stellar populations: one young and one old. If so, the kinematic properties of stars above and below the gap are likely to be distinctly different. The bottom panel of figure 3 shows the velocity dispersions of stars in the McQuillan et al. (2014) sample, with stars subdivided into three groups: those that rotate more quickly than the main rotation period population (green triangles), those with rotation periods shorter than the gap (orange squares), and those with rotation periods longer than the gap (blue circles). Stars were separated into these three groups using Angus et al. (2019) gyrochronology model, according to the scheme shown in the legend. Only stars cooler than 5000 K are included in the bottom panel in order to isolate populations above and below the period gap, which only extends up to a temperature of $\sim$4600 K in our sample (Although Davenport 2017, found that the gap extends to temperatures as hot as 6000 K). In general, velocity dispersion increases with rotation period because both quantities increase with age. There is a smooth

Fig. 3.— Top: rotation period vs. effective temperature for stars in the McQuillan et al. (2014) sample, separated into three groups. Blue circles show stars with rotation periods longer than the period gap, orange squares show stars with rotation periods shorter than the gap, but longer than the lower edge of the main rotation period distribution, and green triangles show stars with rotation periods shorter than this lower edge. Stars were separated into these three groups using Angus et al. (2019) gyrochronology models, with the scheme shown in the legend. Only stars cooler than 5000 K are plotted in the bottom panel in order to isolate populations above and below the period gap, which only extends up to temperatures of ∼4600 K. Bottom: the velocities of these groups of stars (in the direction of Galactic latitude, b) are shown as a function of rotation period. The black line indicates the velocity standard deviation as a function of period.

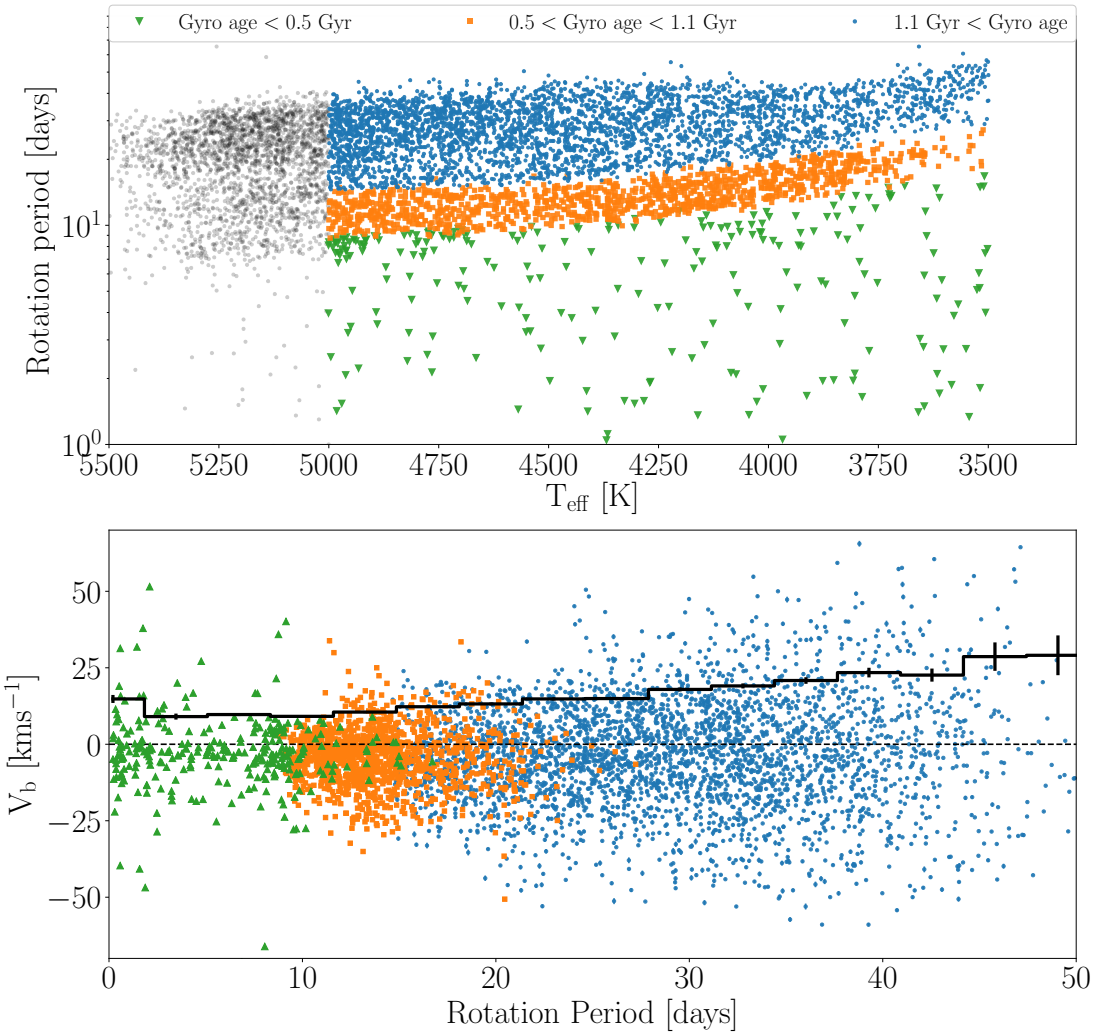

transition in velocity dispersion between stars with rotation periods below and above the gap (orange squares to blue circles), suggesting that these groups are part of the same Galactic population. Previously, only the overall velocity dispersions of all stars above and below the gap have been compared, leading to the assumption that these groups belong to two distinct populations (McQuillan et al. 2014). The smooth increase in velocity dispersion across the gap shown here supports the hypothesis that the gap is caused by a phenomenon of magnetic or structural stellar evolution, not a discontinuity in the local star formation history.

Synchronized binaries are pairs of stars whose rotation periods are equal to their orbital period. Since synchronization appears to happen at rotation periods of 7 days or shorter (Simonian et al. 2019), and most isolated stars have rotation periods longer than 7 days, the rotation periods of synchronized binaries are likely to be *shorter* than they would be if they were isolated stars. For this reason, their rotation periods do not reflect their ages and the gyrochronal age of a synchronized binary is likely to be much younger than the true age of the system. Synchronized binaries are therefore a source of contamination for gyrochronology and should be removed from samples before performing a gyrochronal age analysis. Figure 3 shows that some of the most rapidly rotating stars in the McQuillan et al. (2014) sample have relatively large absolute velocities, indicating that they are likely synchronized binaries. For this reason, the velocity dispersions of stars with rotation periods shorter than the lower edge of the rotation period distribution (green triangles in figure 3) are not significantly smaller than the, presumed older, orange-colored stars. In general, stars with rotation periods less than $\sim$10 days have an increased chance of being synchronized binaries. This result is in agreement with a recent study which found that a large fraction of photometric binaries were rapid rotators, and the probability of a star being a synchronized binary system substantially increased below rotation periods of around 7 days (Simonian et al. 2019). We caution users of rotation period catalogs that rapid rotators with large absolute velocities should be flagged as potential synchronized binaries before applying any gyrochronal analysis.

4. Conclusions

In this paper, we used the $v_{\mathbf{b}}$ velocity dispersions of stars in the McQuillan et al. (2014) catalog to explore the evolution of stellar rotation period as a function of effective temperature and age. Our conclusions are as follows:

- **Magnetic braking efficiency doesn't always increase with decreasing mass for K dwarfs.** Although at young ages, rotation period is anti-correlated with $T_{\rm eff}$ (as seen in many young open clusters, include Praesepe), at intermediate ages the relation flattens out and K dwarfs of different masses rotate at the same rate. At old ages, cooler K dwarfs spin more rapidly than hotter K dwarfs of the same age.

- **Variable core-envelope coupling may be the cause.** We showed that the period–$T_{\rm eff}$ relations change shape over time in a way that qualitatively agrees with theoretical models which include mass and time-dependent core-envelope angular momentum transport (Spada and Lanzafame 2019).

- **Low-mass stars stay active longer.** We found that the oldest stars in the McQuillan et al. (2014) catalog are cooler than 4500 K, which suggests that lower-mass stars remain active for longer, allowing their rotation periods to be measured at older ages.

- **The *Kepler* period gap may be related to core-envelope coupling.** We speculated that the rotation period gap (McQuillan et al. 2014) may separate a young regime where stellar rotation periods decrease with increasing mass from an old regime where periods increase with increasing mass, however more data are needed to provide a conclusive result. The velocity dispersions of stars increase smoothly across the rotation period gap, indicating that the gap does not separate two distinct stellar populations.

- **Rapidly rotating stars with large absolute velocities may be synchronized binaries.** We used kinematics to indicate that there is a population of synchronized binaries with rotation periods less than around 10 days.

- **$\sigma_{v\mathbf{b}}$ can be used as an age proxy for *Kepler* stars.** In the appendix of this paper we demonstrate that the dispersion of velocities in the direction of Galactic latitude, $v_{\mathbf{b}}$, can be used as an age proxy, by showing that there is no strong evidence for mass-dependent heating in low-mass *Kepler* dwarfs: the velocity dispersions of K and M dwarfs, whose main-sequence lifetimes are longer than around 11 Gyrs, do not appear to increase with decreasing mass. Although *vertical* velocity, $v_{\mathbf{z}}$, is a quantity that has been demonstrated to trace time-dependent orbital heating in the disc of the Galaxy, most stars with measured rotation periods do not yet have radial velocities,

so we used velocity in the direction of Galactic latitude, $v_{\mathbf{b}}$ as a proxy for $v_{\mathbf{z}}$. Using stars in the GUMS simulation (Robin et al. 2012), we showed that using $v_{\mathbf{b}}$ as a proxy for $v_{\mathbf{z}}$ introduces an additional pseudo-velocity dispersion, which increases with increasing Galactic latitude. However, after removing high-latitude ($b > 15°$) stars from the sample, we confirmed that using $v_{\mathbf{b}}$ instead of $v_{\mathbf{z}}$ does not introduce any mass-dependent velocity dispersion bias into the sample. We therefore confirmed that $v_{\mathbf{b}}$ velocity dispersion can be used to accurately rank stars by age.

This work was partly developed at the 2019 KITP conference 'Better stars, better planets'. Parts of this project are based on ideas explored at the Gaia sprints at the Flatiron Institute in New York City, 2016 and MPIA, Heidelberg, 2017.

This work made use of the gaia-kepler.fun crossmatch database created by Megan Bedell.

Some of the data presented in this paper were obtained from the Mikulski Archive for Space Telescopes (MAST). STScI is operated by the Association of Universities for Research in Astronomy, Inc., under NASA contract NAS5-26555. Support for MAST for non-HST data is provided by the NASA Office of Space Science via grant NNX09AF08G and by other grants and contracts. This paper includes data collected by the Kepler mission. Funding for the *Kepler* mission is provided by the NASA Science Mission directorate.

This work has made use of data from the European Space Agency (ESA) mission *Gaia* (`https://www.cosmos.esa.int/gaia`), processed by the *Gaia* Data Processing and Analysis Consortium (DPAC, `https://www.cosmos.esa.int/web/gaia/dpac/consortium`). Funding for the DPAC has been provided by national institutions, in particular the institutions participating in the *Gaia* Multilateral Agreement.

5. Appendix: Validating $v_{\mathbf{b}}$ dispersion as an age proxy

The conclusions drawn in this paper depend on the assumption that velocity dispersion in the direction of Galactic latitude ($\sigma_{v\mathbf{b}}$) can be used as an age proxy. There are two main reasons however, why $v_{\mathbf{b}}$ velocity dispersion may *not* be a good age proxy. Firstly, mass-dependent heating may act on the sample, meaning that velocity dispersion depends on both age and mass, so cannot be interpreted as a simple age proxy. Secondly, since stars in the *Kepler* field have a range of Galactic latitudes, using $v_{\mathbf{b}}$ as a stand-in for $v_{\mathbf{z}}$ may not be equally valid for all stars, and introduce a velocity bias for high latitude stars (which are more likely to be cooler and older). In this section we demonstrate that neither of these problems seem to be a significant issue for our data.

In order to establish whether $\sigma_{v\mathbf{b}}$ can be used as an age proxy, we searched for signs of mass-dependent heating within the *Kepler* field. Mass-dependent dynamical heating may result from lower-mass stars experiencing greater velocity changes when gravitationally perturbed than more massive stars. It has not been unambiguously observed in the galactic disk because of the strong anti-correlation between stellar mass and stellar age. Less massive stars do indeed have larger velocity dispersions, however they are also older on average. This mass-age degeneracy is highly reduced in M dwarfs because their main-sequence lifetimes are longer than the age of the Universe, and no evidence for mass-dependent heating has previously been found in M dwarfs (*e.g.* Faherty et al. 2009; Newton et al. 2016).

To investigate whether mass-dependent heating could be acting on the *Kepler* sample, we selected late K and M dwarfs observed by both *Kepler* and *Gaia*, whose MS lifetimes exceed around 11 Gyr and are therefore representative of the initial mass function. We could not perform this analysis on the McQuillan et al. (2014) sample, because it only includes stars with *detectable* rotation periods, and since lower-mass stars stay active for longer it is likely that it contains a strong mass-age correlation. We selected all *Kepler* targets with dereddened *Gaia* $G_{BP} - G_{RP}$ colors greater than 1.2 (corresponding to an effective temperature $\lesssim 4800$ K) and absolute *Gaia* G-band magnitudes < 4. We also eliminated photometric binaries by removing stars above a 6th order polynomial, fit to the MS on the *Gaia* CMD (similar to the one shown in figure 1). We then applied the quality cuts described above in section 2.1. To search for evidence of mass-dependent heating we calculated the ($v_{\mathbf{b}}$) velocity dispersion of stars in effective temperature bins. Sigma clipping was performed at 3σ to remove high and low velocity outliers before calculating the standard deviation of stars in each bin. These extreme velocity outliers may be very old late K and M dwarfs, or they result from using $v_{\mathbf{b}}$ instead of $v_{\mathbf{z}}$, which introduces additional velocity scatter.

Figure 4 shows velocity and velocity dispersion as a function of effective temperature for the K and M *Kepler* dwarf sample. Velocity dispersion very slightly *decreases* with decreasing

temperature, the opposite of the trend expected for mass-dependent heating, however the slope is only inconsistent with zero at 1.3 σ. This trend may be due to a selection bias: cooler stars are fainter and therefore typically closer, with smaller heights above the galactic plane and smaller velocities. The essential point however, is that we do not see evidence for mass-dependent heating acting on stars in the *Kepler* field, indicating that velocity dispersion *can* be used as an age proxy (with the caveat that there is still a chance, albeit a small one, that the opposing effects of the selection function and mass-dependent heating are working to cancel each other out). This analysis was performed using $v_{\mathbf{b}}$ but we also examined the *vertical* velocities of the 537 stars in this sample with RV measurements. Again, no evidence was found for mass-dependent heating: the slope of the velocity dispersion-temperature relation was consistent with zero.

Having found no strong evidence for mass-dependent heating, we next tested the validity of $v_{\mathbf{b}}$ as a proxy for $v_{\mathbf{z}}$ in more detail. At a galactic latitude, b, of zero, $v_b = v_z$, however for increasing values of b, this equivalence becomes an approximation that grows noisier with b. To test the validity of the $v_{\mathbf{b}} \sim v_{\mathbf{z}}$ approximation over a range of latitudes we downloaded stellar data from the *Gaia* Universe Model Snapshot (GUMS) simulation – a simulated *Gaia* catalog (Robin et al. 2012). We downloaded stars from four pointings in the *Kepler* field with galactic latitudes of around 5°, 10°, 15°, and 20°, out to a limiting magnitude of 16 dex, and calculated their $v_{\mathbf{z}}$ and $v_{\mathbf{b}}$ velocities. The relationship between $v_{\mathbf{z}}$ and $v_{\mathbf{b}}$ is close to 1:1, with $v_{\mathbf{z}}$ greater than $v_{\mathbf{b}}$ by around 4.5 kms^{-1} at $b = 5$, due to the Sun's own motion in the Galaxy. We subtracted this offset and examined the residuals of the $v_{\mathbf{z}}$ – $v_{\mathbf{b}}$ relationship to investigate the variance as a function of Galactic latitude (shown in figure 5). We found that $v_{\mathbf{b}}$ is drawn from a heavy-tailed distribution, centered on $v_{\mathbf{z}}$, with standard deviation increasing with b (see figure 5). The standard deviation of $v_{\mathbf{z}}$-$v_{\mathbf{b}}$ was around 3kms^{-1} at $b \sim 5°$, 4kms^{-1} at 10°, 6kms^{-1} at 15°, and 9kms^{-1} at 20°. This demonstrates that using $v_{\mathbf{b}}$ instead of $v_{\mathbf{z}}$ for stars in the *Kepler* field will introduce an additional velocity scatter, inflating $\sigma_{v\mathbf{b}}$ relative to $\sigma_{v\mathbf{z}}$. This additional velocity scatter will be greatest for stars at the highest Galactic latitudes.

Since we are concerned with velocity *dispersions*, rather than velocities themselves, we also compared $\sigma_{v\mathbf{b}}$ and $\sigma_{v\mathbf{z}}$ as a function of temperature for stars downloaded from the GUMS simulation. For stars at galactic latitudes of 15° or less, $\sigma_{v\mathbf{b}}$ was consistent with $\sigma_{v\mathbf{z}}$, within uncertainties, however, at higher latitudes the two quantities became significantly different. For this reason we proceeded by only including stars with galactic latitudes less than 15° in our analysis. Although we find that the transformation between $v_{\mathbf{z}}$ and $v_{\mathbf{b}}$ does not *strongly* affect our results, we cannot rule out the possibility that it introduces systematic biases into the velocity dispersions we present here. In *Gaia* DR3, RVs will be available for most stars in this sample, providing an opportunity to validate (or correct) the results presented here,

Fig. 4.— Top: Stellar velocity ($v_{\mathbf{b}}$) as a function of $T_{\rm eff}$ for *Kepler* K and M dwarfs. Vertical lines indicate different $T_{\rm eff}$-groupings used to calculate velocity dispersion. Pink stars were not included in velocity dispersion calculations as they were either removed as outliers during a sigma clipping process, or they lie at the sparcely populated, extremely cool end of the temperature range. Velocity dispersion and $T_{\rm eff}$ are slightly positively correlated, likely due to a brightness-related selection bias, indicating that mass-dependent heating does not significantly affect low-mass stars in the *Kepler* field.

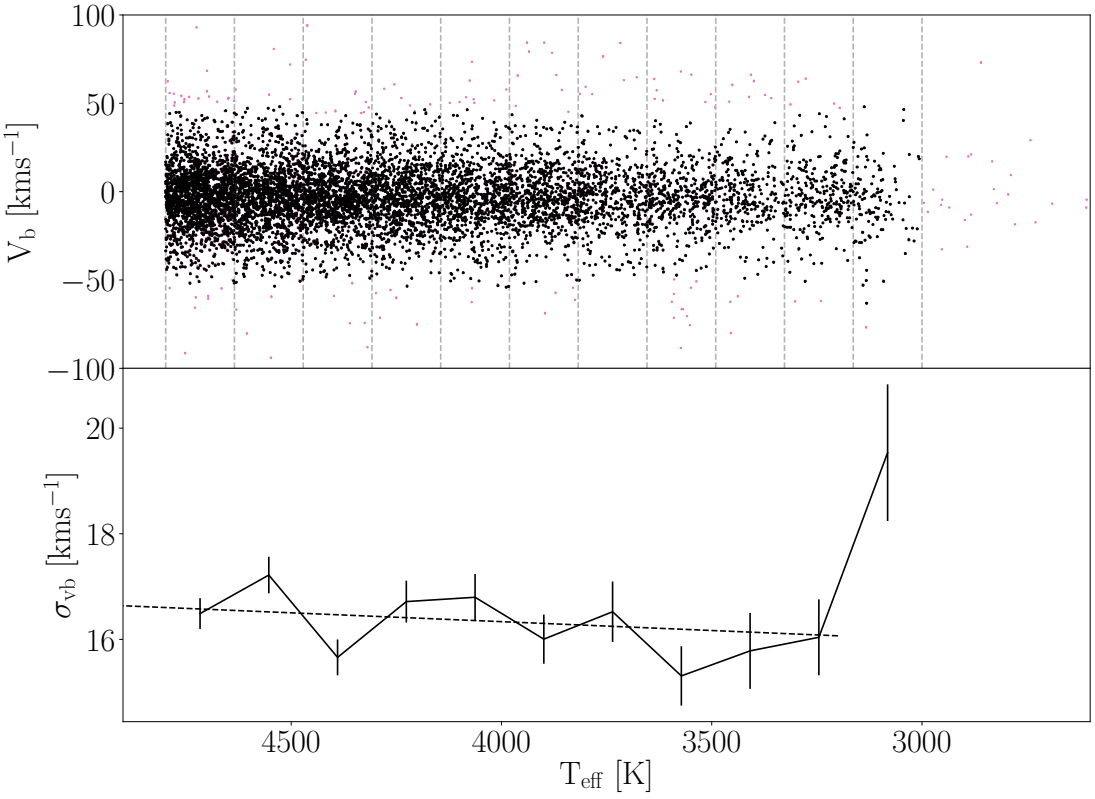

and to work in action-space, rather than velocity-space.

Because of the noisy relationship between $v_{\mathbf{b}}$ and $v_{\mathbf{z}}$ in this paper we do not attempt to convert velocity dispersion ($\sigma_{v\mathbf{b}}$) into an age via an age-velocity dispersion relation (AVR) (*e.g.* Holmberg et al. 2009). Although we find that $\sigma_{v\mathbf{b}}$ can be used to rank groups of stars by age, a more careful analysis that includes formal modeling of the $v_{\mathbf{b}} - v_{\mathbf{z}}$ relationship will be needed to calculate absolute ages.

Fig. 5.— This figure demonstrates the variance in the relationship between $v_{\mathbf{b}}$ and $v_{\mathbf{z}}$ for stars in the *Kepler* field, based on the GUMS simulation. The panels show a kernel density estimator (KDE) (black solid line) for the $v_{\mathbf{z}}$– $v_{\mathbf{b}}$ residuals of stars in the GUMS simulation at four different Galactic latitudes. Blue dashed lines show Gaussian fits to these KDEs. The distributions are close to Gaussian, with slightly heavy tails. The standard deviations of the Gaussian fits increase with Galactic latitude. This figure illustrates how using $v_{\mathbf{b}}$ instead of $v_{\mathbf{z}}$ artificially increases velocity dispersion, especially at high latitudes.

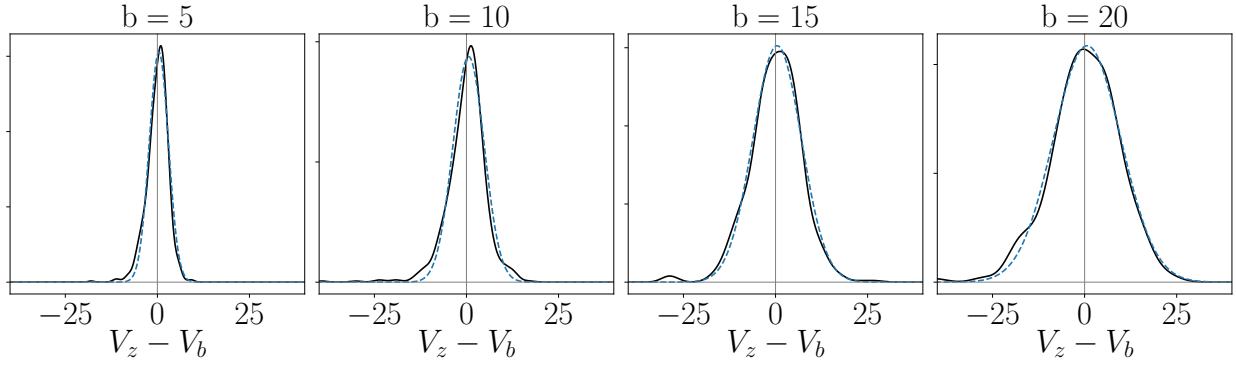

REFERENCES

R. Angus, S. Aigrain, D. Foreman-Mackey, and A. McQuillan. Calibrating gyrochronology using Kepler asteroseismic targets. *MNRAS*, 450:1787–1798, June 2015. doi: 10.1093/mnras/stv423.

Ruth Angus et al. Towards precise stellar ages: combining isochrone fitting with empirical gyrochronology. *AJ*, 2019.

Astropy Collaboration, T. P. Robitaille, E. J. Tollerud, P. Greenfield, M. Droettboom, E. Bray, T. Aldcroft, M. Davis, A. Ginsburg, A. M. Price-Whelan, W. E. Kerzendorf, A. Conley, N. Crighton, K. Barbary, D. Muna, H. Ferguson, F. Grollier, M. M. Parikh, P. H. Nair, H. M. Unther, C. Deil, J. Woillez, S. Conseil, R. Kramer, J. E. H. Turner, L. Singer, R. Fox, B. A. Weaver, V. Zabalza, Z. I. Edwards, K. Azalee Bostroem, D. J. Burke, A. R. Casey, S. M. Crawford, N. Dencheva, J. Ely, T. Jenness, K. Labrie, P. L. Lim, F. Pierfederici, A. Pontzen, A. Ptak, B. Refsdal, M. Servillat, and O. Streicher. Astropy: A community Python package for astronomy. *A&A*, 558:A33, October 2013. doi: 10.1051/0004-6361/201322068.

M. Aumer and J. J. Binney. Kinematics and history of the solar neighbourhood revisited. *MNRAS*, 397:1286–1301, August 2009. doi: 10.1111/j.1365-2966.2009.15053.x.

Michael Aumer, James Binney, and Ralph Schönrich. Age-velocity dispersion relations and heating histories in disc galaxies. *MNRAS*, 462(2):1697–1713, Oct 2016. doi: 10.1093/mnras/stw1639.

S. A. Barnes. On the Rotational Evolution of Solar- and Late-Type Stars, Its Magnetic Origins, and the Possibility of Stellar Gyrochronology. *ApJ*, 586:464–479, March 2003. doi: 10.1086/367639.

S. A. Barnes. Ages for Illustrative Field Stars Using Gyrochronology: Viability, Limitations, and Errors. *ApJ*, 669:1167–1189, November 2007. doi: 10.1086/519295.

S. A. Barnes. A Simple Nonlinear Model for the Rotation of Main-sequence Cool Stars. I. Introduction, Implications for Gyrochronology, and Color-Period Diagrams. *ApJ*, 722:222–234, October 2010. doi: 10.1088/0004-637X/722/1/222.

Angus Beane, Melissa K. Ness, and Megan Bedell. Actions Are Weak Stellar Age Indicators in the Milky Way Disk. *ApJ*, 867(1):31, Nov 2018. doi: 10.3847/1538-4357/aae07f.

Travis A. Berger, Daniel Huber, Jennifer L. van Saders, Eric Gaidos, Jamie Tayar, and Adam L. Kraus. The *Gaia-Kepler* Stellar Properties Catalog I: Homogeneous Fundamental Properties for 186,000 *Kepler* Stars. *arXiv e-prints*, art. arXiv:2001.07737, January 2020.

Jonathan C. Bird, Stelios Kazantzidis, David H. Weinberg, Javiera Guedes, Simone Callegari, Lucio Mayer, and Piero Madau. Inside out and Upside down: Tracing the Assembly of a Simulated Disk Galaxy Using Mono-age Stellar Populations. *ApJ*, 773(1):43, August 2013. doi: 10.1088/0004-637X/773/1/43.

William J. Borucki, David Koch, Gibor Basri, Natalie Batalha, Timothy Brown, Douglas Caldwell, John Caldwell, Jørgen Christensen-Dalsgaard, William D. Cochran, Edna DeVore, Edward W. Dunham, Andrea K. Dupree, Thomas N. Gautier, John C. Geary, Ronald Gilliland, Alan Gould, Steve B. Howell, Jon M. Jenkins, Yoji Kondo, David W. Latham, Geoffrey W. Marcy, Søren Meibom, Hans Kjeldsen, Jack J. Lissauer, David G. Monet, David Morrison, Dimitar Sasselov, Jill Tarter, Alan Boss, Don Brownlee, Toby Owen, Derek Buzasi, David Charbonneau, Laurance Doyle, Jonathan Fortney, Eric B. Ford, Matthew J. Holman, Sara Seager, Jason H. Steffen, William F. Welsh, Jason Rowe, Howard Anderson, Lars Buchhave, David Ciardi, Lucianne Walkowicz, William Sherry, Elliott Horch, Howard Isaacson, Mark E. Everett, Debra Fischer, Guillermo Torres, John Asher Johnson, Michael Endl, Phillip MacQueen, Stephen T. Bryson, Jessie Dotson, Michael Haas, Jeffrey Kolodziejczak, Jeffrey Van Cleve, Hema Chandrasekaran, Joseph D. Twicken, Elisa V. Quintana, Bruce D. Clarke, Christopher Allen, Jie Li, Haley Wu, Peter Tenenbaum, Ekaterina Verner, Frederick Bruhweiler, Jason Barnes, and Andrej Prsa. Kepler Planet-Detection Mission: Introduction and First Results. *Science*, 327(5968):977, Feb 2010. doi: 10.1126/science.1185402.

Tabetha S. Boyajian, Kaspar von Braun, Gerard van Belle, Harold A. McAlister, Theo A. ten Brummelaar, Stephen R. Kane, Philip S. Muirhead, Jeremy Jones, Russel White, Gail Schaefer, David Ciardi, Todd Henry, Mercedes López-Morales, Stephen Ridgway, Douglas Gies, Wei-Chun Jao, Bárbara Rojas-Ayala, J. Robert Parks, Laszlo Sturmann, Judit Sturmann, Nils H. Turner, Chris Farrington, P. J. Goldfinger, and David H. Berger. Stellar Diameters and Temperatures. II. Main-sequence K- and M-stars. *ApJ*, 757(2):112, October 2012. doi: 10.1088/0004-637X/757/2/112.

John M. Brewer, Debra A. Fischer, Jeff A. Valenti, and Nikolai Piskunov. Spectral Properties of Cool Stars: Extended Abundance Analysis of 1,617 Planet-search Stars. *ApJS*, 225 (2):32, August 2016. doi: 10.3847/0067-0049/225/2/32.

L. Casagrande, R. Schönrich, M. Asplund, S. Cassisi, I. Ramírez, J. Meléndez, T. Bensby, and S. Feltzing. New constraints on the chemical evolution of the solar neighbourhood and Galactic disc(s). Improved astrophysical parameters for the Geneva-Copenhagen Survey. *A&A*, 530:A138, Jun 2011. doi: 10.1051/0004-6361/201016276.

Paul Charbonneau. Dynamo Models of the Solar Cycle. *Living Reviews in Solar Physics*, 7 (1):3, September 2010. doi: 10.12942/lrsp-2010-3.

J. L. Curtis, M. A. Agüeros, S. T. Douglas, and S. Meibom. A Temporary Epoch of Stalled Spin-Down for Low-Mass Stars: Insights from NGC 6811 with Gaia and Kepler. *arXiv e-prints*, May 2019.

James R. A. Davenport. Rotating Stars from Kepler Observed with Gaia DR1. *ApJ*, 835 (1):16, Jan 2017. doi: 10.3847/1538-4357/835/1/16.

James R. A. Davenport and Kevin R. Covey. Rotating Stars from Kepler Observed with Gaia DR2. *ApJ*, 868(2):151, Dec 2018. doi: 10.3847/1538-4357/aae842.

S. T. Douglas, M. A. Agüeros, K. R. Covey, and A. Kraus. Poking the Beehive from Space: K2 Rotation Periods for Praesepe. *ApJ*, 842:83, June 2017. doi: 10.3847/1538-4357/aa6e52.

Jacqueline K. Faherty, Adam J. Burgasser, Kelle L. Cruz, Michael M. Shara, Frederick M. Walter, and Christopher R. Gelino. The Brown Dwarf Kinematics Project I. Proper Motions and Tangential Velocities for a Large Sample of Late-Type M, L, and T Dwarfs. *AJ*, 137(1):1–18, Jan 2009. doi: 10.1088/0004-6256/137/1/1.

F. Gallet and J. Bouvier. Improved angular momentum evolution model for solar-like stars. *A&A*, 556:A36, Aug 2013. doi: 10.1051/0004-6361/201321302.

R. A. García, T. Ceillier, D. Salabert, S. Mathur, J. L. van Saders, M. Pinsonneault, J. Ballot, P. G. Beck, S. Bloemen, T. L. Campante, G. R. Davies, Jr. do Nascimento, J. D., S. Mathis, T. S. Metcalfe, M. B. Nielsen, J. C. Suárez, W. J. Chaplin, A. Jiménez, and C. Karoff. Rotation and magnetism of Kepler pulsating solar-like stars. Towards asteroseismically calibrated age-rotation relations. *A&A*, 572:A34, Dec 2014. doi: 10.1051/0004-6361/201423888.

J. Holmberg, B. Nordström, and J. Andersen. The Geneva-Copenhagen survey of the Solar neighbourhood II. New uvby calibrations and rediscussion of stellar ages, the G dwarf problem, age-metallicity diagram, and heating mechanisms of the disk. *A&A*, 475: 519–537, November 2007. doi: 10.1051/0004-6361:20077221.

J. Holmberg, B. Nordström, and J. Andersen. The Geneva-Copenhagen survey of the solar neighbourhood. III. Improved distances, ages, and kinematics. *A&A*, 501:941–947, July 2009. doi: 10.1051/0004-6361/200811191.

Steve B. Howell, Charlie Sobeck, Michael Haas, Martin Still, Thomas Barclay, Fergal Mullally, John Troeltzsch, Suzanne Aigrain, Stephen T. Bryson, Doug Caldwell, William J. Chaplin, William D. Cochran, Daniel Huber, Geoffrey W. Marcy, Andrea Miglio, Joan R. Najita, Marcie Smith, J. D. Twicken, and Jonathan J. Fortney. The K2 Mission: Characterization and Early Results. *PASP*, 126(938):398, Apr 2014. doi: 10.1086/676406.

Jonathan Irwin and Jerome Bouvier. The rotational evolution of low-mass stars. In Eric E. Mamajek, David R. Soderblom, and Rosemary F. G. Wyse, editors, *The Ages of Stars*, volume 258 of *IAU Symposium*, pages 363–374, Jun 2009. doi: 10.1017/S1743921309032025.

Kenneth A. Janes and Sadia Hoq. A Quantitative Analysis of Distant Open Clusters. *AJ*, 141(3):92, March 2011. doi: 10.1088/0004-6256/141/3/92.

S. D. Kawaler. Angular momentum loss in low-mass stars. *ApJ*, 333:236–247, October 1988. doi: 10.1086/166740.

Rocio Kiman, Sarah J. Schmidt, Ruth Angus, Kelle L. Cruz, Jacqueline K. Faherty, and Emily Rice. Exploring the Age-dependent Properties of M and L Dwarfs Using Gaia and SDSS. *AJ*, 157(6):231, Jun 2019. doi: 10.3847/1538-3881/ab1753.

Gregory M. Green. dustmaps: A Python interface for maps of interstellar dust. *The Journal of Open Source Software*, 3(26):695, Jun 2018. doi: 10.21105/joss.00695.

Andrew W. Mann, Gregory A. Feiden, Eric Gaidos, Tabetha Boyajian, and Kaspar von Braun. How to Constrain Your M Dwarf: Measuring Effective Temperature, Bolometric Luminosity, Mass, and Radius. *ApJ*, 804(1):64, May 2015. doi: 10.1088/0004-637X/804/1/64.

Marie Martig, Ivan Minchev, and Chris Flynn. Dissecting simulated disc galaxies - II. The age-velocity relation. *MNRAS*, 443(3):2452–2462, Sep 2014. doi: 10.1093/mnras/stu1322.

A. McQuillan, S. Aigrain, and T. Mazeh. Measuring the rotation period distribution of field M dwarfs with Kepler. *MNRAS*, 432(2):1203–1216, Jun 2013. doi: 10.1093/mnras/stt536.

A. McQuillan, T. Mazeh, and S. Aigrain. Rotation Periods of 34,030 Kepler Main-sequence Stars: The Full Autocorrelation Sample. *ApJS*, 211:24, April 2014. doi: 10.1088/0067-0049/211/2/24.

S. Meibom, S. A. Barnes, D. W. Latham, N. Batalha, W. J. Borucki, D. G. Koch, G. Basri, L. M. Walkowicz, K. A. Janes, J. Jenkins, J. Van Cleve, M. R. Haas, S. T. Bryson, A. K. Dupree, G. Furesz, A. H. Szentgyorgyi, L. A. Buchhave, B. D. Clarke, J. D. Twicken, and E. V. Quintana. The Kepler Cluster Study: Stellar Rotation in NGC 6811. *ApJ*, 733:L9, May 2011. doi: 10.1088/2041-8205/733/1/L9.

S. Meibom, S. A. Barnes, I. Platais, R. L. Gilliland, D. W. Latham, and R. D. Mathieu. A spin-down clock for cool stars from observations of a 2.5-billion-year-old cluster. *Nature*, 517:589–591, January 2015. doi: 10.1038/nature14118.

Travis S. Metcalfe and Ricky Egeland. Understanding the Limitations of Gyrochronology for Old Field Stars. *ApJ*, 871(1):39, Jan 2019. doi: 10.3847/1538-4357/aaf575.

Elisabeth R. Newton, Jonathan Irwin, David Charbonneau, Zachory K. Berta-Thompson, Jason A. Dittmann, and Andrew A. West. The Rotation and Galactic Kinematics of Mid M Dwarfs in the Solar Neighborhood. *ApJ*, 821(2):93, Apr 2016. doi: 10.3847/0004-637X/821/2/93.

Elisabeth R. Newton, Jonathan Irwin, David Charbonneau, Perry Berlind, Michael L. Calkins, and Jessica Mink. The Hα Emission of Nearby M Dwarfs and its Relation to Stellar Rotation. *ApJ*, 834(1):85, January 2017. doi: 10.3847/1538-4357/834/1/85.

Elisabeth R. Newton, Nicholas Mondrik, Jonathan Irwin, Jennifer G. Winters, and David Charbonneau. New Rotation Period Measurements for M Dwarfs in the Southern Hemisphere: An Abundance of Slowly Rotating, Fully Convective Stars. *AJ*, 156(5):217, November 2018. doi: 10.3847/1538-3881/aad73b.

B. Nordström, M. Mayor, J. Andersen, J. Holmberg, F. Pont, B. R. Jørgensen, E. H. Olsen, S. Udry, and N. Mowlavi. The Geneva-Copenhagen survey of the Solar neighbourhood. Ages, metallicities, and kinematic properties of 14 000 F and G dwarfs. *A&A*, 418:989–1019, May 2004. doi: 10.1051/0004-6361:20035959.

R. W. Noyes, L. W. Hartmann, S. L. Baliunas, D. K. Duncan, and A. H. Vaughan. Rotation, convection, and magnetic activity in lower main-sequence stars. *ApJ*, 279:763–777, April 1984. doi: 10.1086/161945.

E. N. Parker. The Generation of Magnetic Fields in Astrophysical Bodies. I. The Dynamo Equations. *ApJ*, 162:665, November 1970. doi: 10.1086/150697.

M. H. Pinsonneault, S. D. Kawaler, S. Sofia, and P. Demarque. Evolutionary models of the rotating sun. *ApJ*, 338:424–452, March 1989. doi: 10.1086/167210.

A. M. Price-Whelan, B. M. Sipőcz, H. M. Günther, P. L. Lim, S. M. Crawford, S. Conseil, D. L. Shupe, M. W. Craig, N. Dencheva, A. Ginsburg, J. T. VanderPlas, L. D. Bradley, D. Pérez-Suárez, M. de Val-Borro, (Primary Paper Contributors, T. L. Aldcroft, K. L. Cruz, T. P. Robitaille, E. J. Tollerud, (Astropy Coordination Committee, C. Ardelean, T. Babej, Y. P. Bach, M. Bachetti, A. V. Bakanov, S. P. Bamford, G. Barentsen, P. Barmby, A. Baumbach, K. L. Berry, F. Biscani, M. Boquien, K. A. Bostroem, L. G. Bouma, G. B. Brammer, E. M. Bray, H. Breytenbach, H. Buddelmeijer, D. J. Burke, G. Calderone, J. L. Cano Rodríguez, M. Cara, J. V. M. Cardoso, S. Cheedella, Y. Copin, L. Corrales, D. Crichton, D. D'Avella, C. Deil, É. Depagne, J. P. Dietrich, A. Donath, M. Droettboom, N. Earl, T. Erben, S. Fabbro, L. A. Ferreira, T. Finethy, R. T. Fox, L. H. Garrison, S. L. J. Gibbons, D. A. Goldstein, R. Gommers, J. P. Greco, P. Greenfield, A. M. Groener, F. Grollier, A. Hagen, P. Hirst, D. Homeier, A. J. Horton, G. Hosseinzadeh, L. Hu, J. S. Hunkeler, Ž. Ivezić, A. Jain, T. Jenness, G. Kanarek, S. Kendrew, N. S. Kern, W. E. Kerzendorf, A. Khvalko, J. King, D. Kirkby, A. M. Kulkarni, A. Kumar, A. Lee, D. Lenz, S. P. Littlefair, Z. Ma, D. M. Macleod, M. Mastropietro, C. McCully, S. Montagnac, B. M. Morris, M. Mueller, S. J. Mumford, D. Muna, N. A. Murphy, S. Nelson, G. H. Nguyen, J. P. Ninan, M. Nöthe, S. Ogaz, S. Oh, J. K. Parejko, N. Parley, S. Pascual, R. Patil, A. A. Patil, A. L. Plunkett, J. X. Prochaska, T. Rastogi, V. Reddy Janga, J. Sabater, P. Sakurikar, M. Seifert, L. E. Sherbert, H. Sherwood-Taylor, A. Y. Shih, J. Sick, M. T. Silbiger, S. Singanamalla, L. P. Singer, P. H. Sladen, K. A. Sooley, S. Sornarajah, O. Streicher, P. Teuben, S. W. Thomas, G. R. Tremblay, J. E. H. Turner, V. Terrón, M. H. van Kerkwijk, A. de la Vega, L. L. Watkins, B. A. Weaver, J. B. Whitmore, J. Woillez, V. Zabalza, and (Astropy) Contributors. The Astropy Project: Building an Open-science Project and Status of the v2.0 Core Package. *AJ*, 156:123, September 2018. doi: 10.3847/1538-3881/aabc4f.

Adrian Price-Whelan. adrn/pyia: v0.2. Apr 2018. doi: 10.5281/zenodo.1228136.

Markus Rabus, Régis Lachaume, Andrés Jordán, Rafael Brahm, Tabetha Boyajian, Kaspar von Braun, Néstor Espinoza, Jean-Philippe Berger, Jean-Baptiste Le Bouquin, and Olivier Absil. A discontinuity in the T_{eff}-radius relation of M-dwarfs. *MNRAS*, 484 (2):2674–2683, April 2019. doi: 10.1093/mnras/sty3430.

L. M. Rebull, J. R. Stauffer, L. A. Hillenbrand, A. M. Cody, J. Bouvier, D. R. Soderblom, M. Pinsonneault, and L. Hebb. Rotation of Late-type Stars in Praesepe with K2. *ApJ*, 839:92, April 2017. doi: 10.3847/1538-4357/aa6aa4.

Timo Reinhold, Keaton J. Bell, James Kuszlewicz, Saskia Hekker, and Alexander I. Shapiro. Transition from spot to faculae domination. An alternate explanation for the dearth of intermediate Kepler rotation periods. *A&A*, 621:A21, Jan 2019. doi: 10.1051/0004-6361/201833754.

A. C. Robin, X. Luri, C. Reylé, Y. Isasi, E. Grux, S. Blanco-Cuaresma, F. Arenou, C. Babusiaux, M. Belcheva, R. Drimmel, C. Jordi, A. Krone-Martins, E. Masana, J. C. Mauduit, F. Mignard, N. Mowlavi, B. Rocca-Volmerange, P. Sartoretti, E. Slezak, and A. Sozzetti. Gaia Universe model snapshot. A statistical analysis of the expected contents of the Gaia catalogue. *A&A*, 543:A100, Jul 2012. doi: 10.1051/0004-6361/201118646.

E. Schatzman. A theory of the role of magnetic activity during star formation. *Annales d'Astrophysique*, 25:18, February 1962.

J. A. Sellwood. Secular evolution in disk galaxies. *Reviews of Modern Physics*, 86(1):1–46, Jan 2014. doi: 10.1103/RevModPhys.86.1.

Gregory V. A. Simonian, Marc H. Pinsonneault, and Donald M. Terndrup. Rapid Rotation in the Kepler Field: Not a Single Star Phenomenon. *ApJ*, 871(2):174, Feb 2019. doi: 10.3847/1538-4357/aaf97c.

A. Skumanich. Time Scales for CA II Emission Decay, Rotational Braking, and Lithium Depletion. *ApJ*, 171:565, February 1972. doi: 10.1086/151310.

F. Spada and A. C. Lanzafame. On the competing effect of wind braking and interior coupling in the rotational evolution of solar-like stars. *arXiv e-prints*, art. arXiv:1908.00345, Aug 2019.

Antony A. Stark and Jan Brand. Kinematics of Molecular Clouds. II. New Data on Nearby Giant Molecular Clouds. *ApJ*, 339:763, Apr 1989. doi: 10.1086/167334.

Antony A. Stark and Youngung Lee. The Scale Height of Giant Molecular Clouds Is Less than That of Smaller Clouds. *ApJ*, 619(2):L159–L162, Feb 2005. doi: 10.1086/427936.

Yuan-Sen Ting and Hans-Walter Rix. The Vertical Motion History of Disk Stars throughout the Galaxy. *ApJ*, 878(1):21, Jun 2019. doi: 10.3847/1538-4357/ab1ea5.

J. L. van Saders, T. Ceillier, T. S. Metcalfe, V. Silva Aguirre, M. H. Pinsonneault, R. A. García, S. Mathur, and G. R. Davies. Weakened magnetic braking as the origin of anomalously rapid rotation in old field stars. *Nature*, 529:181–184, January 2016. doi: 10.1038/nature16168.

J. L. van Saders, M. H. Pinsonneault, and M. Barbieri. Forward Modeling of the Kepler Stellar Rotation Period Distribution: Interpreting Periods from Mixed and Biased Stellar Populations. *ArXiv e-prints*, March 2018.

E. J. Weber and L. Davis, Jr. The Angular Momentum of the Solar Wind. *ApJ*, 148:217–227, April 1967. doi: 10.1086/149138.

Andrew A. West, Suzanne L. Hawley, John J. Bochanski, Kevin R. Covey, I. Neill Reid, Saurav Dhital, Eric J. Hilton, and Michael Masuda. Constraining the Age-Activity Relation for Cool Stars: The Sloan Digital Sky Survey Data Release 5 Low-Mass Star Spectroscopic Sample. *AJ*, 135(3):785–795, Mar 2008. doi: 10.1088/0004-6256/135/3/785.

Andrew A. West, Dylan P. Morgan, John J. Bochanski, Jan Marie Andersen, Keaton J. Bell, Adam F. Kowalski, James R. A. Davenport, Suzanne L. Hawley, Sarah J. Schmidt, David Bernat, Eric J. Hilton, Philip Muirhead, Kevin R. Covey, Bárbara Rojas-Ayala, Everett Schlawin, Mary Gooding, Kyle Schluns, Saurav Dhital, J. Sebastian Pineda, and David O. Jones. The Sloan Digital Sky Survey Data Release 7 Spectroscopic M Dwarf Catalog. I. Data. *AJ*, 141(3):97, Mar 2011. doi: 10.1088/0004-6256/141/3/97.